PERGAMON

International Journal of Heat and Mass Transfer 41 (1998) 3635–3645

International Journal of HEAT and MASS TRANSFER

Numerical and experimental study of transient turbulent natural convection in a horizontal cylindrical container

J. L. Xia[a,*], B. L. Smith[b], G. Yadigaroglu[a], U. Gantner[a], B. Sigg[a]

[a] *Nuclear Engineering Laboratory, Swiss Federal Institute of Technology, ETH-Zentrum, CLT, CH-8092 Zurich, Switzerland*
[b] *Thermal Hydraulics Laboratory, Paul Scherrer Institute, CH-5232 Villigen PSI, Switzerland*

Received 4 March 1997; in final form 28 August 1997

Abstract

Transient, turbulent, natural convection in a horizontal cylindrical container is numerically and experimentally investigated. The container is of aluminium, filled with water,and a piece-wise constant heat flux is imposed on the outside wall. Numerical results show that there exist conduction-controlled, developing and quasi-steady-state periods during the transient and that the existence of the wall has some influence on the flow and heat transfer. The flow undergoes two-vortex, four-vortex and then again two-vortex configuration changes during the transient. The four-vortex flow pattern appears to be relatively unstable, and is accompanied by asymmetric flow in the bottom region of the container. Both numerical predictions and experiments reveal a well-stratified thermal field and numerical results are validated against experimental data.

Key words: Conjugate; Transient; Turbulent; Natural convection; Horizontal cylindrical container

Nomenclature

C's empirical constants in the turbulence model
D_i, D_o inner and outer cylinder diameter
G buoyancy effect
k turbulence kinetic energy
Nu Nusselt number
P production term
Pr molecular Prandtl number
q_w externally-imposed wall heat flux
Ra Rayleigh number
T temperature
u_i mean velocity in the x_i-direction
x_i spatial coordinate in the i-direction.

Greek symbols
α thermal diffusivity
ε dissipation rate of k
λ thermal conductivity
μ dynamic viscosity
μ_t turbulent viscosity
ν kinematic viscosity
σs empirical diffusion coefficients in the turbulence model
ρ density.

Subscripts
i, j spatial coordinates
f fluid
w wall.

1. Introduction

Natural convection in a horizontal cylindrical container has drawn attention as early as the 1950s. A number of researchers have studied this problem, either theoretically, experimentally or both. Martini and Churchill [1] experimentally examined laminar flow and heat transfer in a horizontal cylinder heated from the two sides and found that the core region is thermally-stratified and relatively stagnant. the situation of sinusoidal wall heating, with changing phase angle, was experimentally

* Corresponding author. Permanent address: Institute of Engineering Thermophysics, Chongqing University, Chongqing 630044, China.

0017–9310/98 $19.00
PII: S0017–9310(97)00297–4

investigated by Sabzerari and Ostrach [2], ranging from heating from the side to heating from below. Natural convection induced in a horizontal cylinder by linear temperature boundary conditions was studied experimentally by Brook and Ostrach [3]. Deaver and Eckert [4] reported interferometric results of the transient convection in a horizontal cylinder with increasing wall temperature. Theoretical analyses include those of Weinbaum [5] and Ostrach and Hantman [6]. The first numerical solution for this problem appears to be by Hellums and Churchill [7], which is the companion work to the Martini and Churchill experiments. Robiland et al. [8] examined the influence of time-dependent boundary conditions. Takeuch and Cheng [9] studied laminar convective heat transfer in horizontal tubes with decreasing wall temperature. Leong and Davis [10] reported a numerical study of steady-state natural convection at different heating phase angles. Recently, Xia et al. [11] carried out a numerical investigation for steady/unsteady flow and heat transfer in a horizontal cylinder and found that a nearly-stagnant, thermally-stratified core exists only at moderately high Rayleigh numbers ($Ra_T > 10^5$), and that the time evolution of the flow and thermal fields are Rayleigh-number dependent. An experimental and numerical study of unsteady natural convection in air in a horizontal tube with constant heat generation on the outside wall was conducted by Vatutin et al. [12], who observed the transition of the flow from a two-vortex to four-vortex structure.

Some studies have been also carried out for the transient, laminar, natural convection in a vertical cylinder. These include the work of Lee et al. [13], who numerically studied the transient flow in a partially-filled vertical cylinder with a constant wall temperature, and of Sun and Oosthuizen [14, 15], who examined transient, natural convection flow in a vertical cylinder with a specified wall flux, and with a specified wall temperature.

Though efforts in this field appear extensive, all the past studies have focused on laminar flow and heat transfer, and have also assumed ideal wall boundary conditions (zero wall thickness, constant wall temperature or heat flux, among others). It seems to the present authors that there appears to be no report in the open literature which takes the wall effect into consideration and extends the flow into the turbulent region. In practical situations, most of the flow may be expected to be turbulent and the influence of wall heat conduction may be important, leading to a conjugate, conduction/natural convection problem.

To complement the reported investigations, a numerical study of transient natural circulation in a horizontal cylinder, which includes the effects due to turbulence and wall heat conduction, is obviously in order. This is the theme of the present paper, which extends the Rayleigh number into the turbulent region and presents comparisons between numerical results and experimental data. The present investigation has also been undertaken to study the analogy between volumetric cooling of a depressurizing gas stored in a cylindrical tank and the steady heating of a fluid through the wall of its cylindrical container. Calculations for the volumetric heat sink case have been presented in Ref. [16].

2. Physical model and numerical procedure

The physical model is shown in Fig. 1(a) and consists of a horizontal cylindrical container, made of aluminium, of internal diameter $D = 0.22$ m, of wall thickness $\delta = 0.015$ m, and filled with water. Initially, the fluid inside the container is at rest, and the wall and water inside are at the same uniform temperature $T_i = 20^\circ$C. At time $t = 0$, heat is supplied to the outside of the container wall by means of an imposed heat flux $q_{w1} = 3500$ W m^{-2} along the top quarter sector and $q_{w2} = 7160$ W m^{-2} along the remainder (see Fig. 1(a)). It initiates a heat transfer process from the heated wall to the fluid and drives circulation inside the container. This forms an intricate, transient, conjugate natural convection–conduction problem. For the thermal properties chosen, the Rayleigh number, defined in terms of the outside wall heat flux, is given by

$$Ra = \frac{4\beta g q_w D_i^3 D_o}{\nu \alpha k} = 4.01 \times 10^{12}. \quad (1)$$

In the present calculations, the flow and heat transfer are assumed to be two-dimensional. In order to describe the turbulent flow and heat transfer, a k–ε turbulence model is used. Two-dimensional heat conduction in the container wall is also taken into account, and is fully coupled to the fluid flow calculation. The governing equations for the mean quantities in tensor notation are given below. For the fluid,

$$\frac{\partial \rho}{\partial t} + \frac{\partial (\rho u_j)}{\partial x_j} = 0 \quad (2)$$

$$\frac{\partial (\rho u_i)}{\partial t} + \frac{\partial (\rho u_i u_j)}{\partial x_j} = -\frac{\partial \rho}{\partial x_i} + \frac{\partial}{\partial x_j}\left[(\mu + \mu_t)\left(\frac{\partial u_i}{\partial x_j} + \frac{\partial u_j}{\partial x_i}\right)\right] + (\rho - \rho_o) g_i \quad (3)$$

$$\frac{\partial (\rho T)}{\partial t} + \frac{\partial (\rho u_j T)}{\partial x_j} = \frac{\partial}{\partial x_j}\left[\left(\frac{\mu}{Pr} + \frac{\mu_t}{\sigma_T}\right)\frac{\partial T}{\partial x_j}\right] \quad (4)$$

where ρ is the density, u_j the mean velocity component, x_j the Cartesian coordinate, t the time, Pr the molecular Prandtl number, σ_T the turbulent Prandtl number, Tr the mean temperature, μ the molecular dynamic viscosity and μ_t the turbulent viscosity,which is related to the turbulent kinetic energy k and its dissipation rate ε by

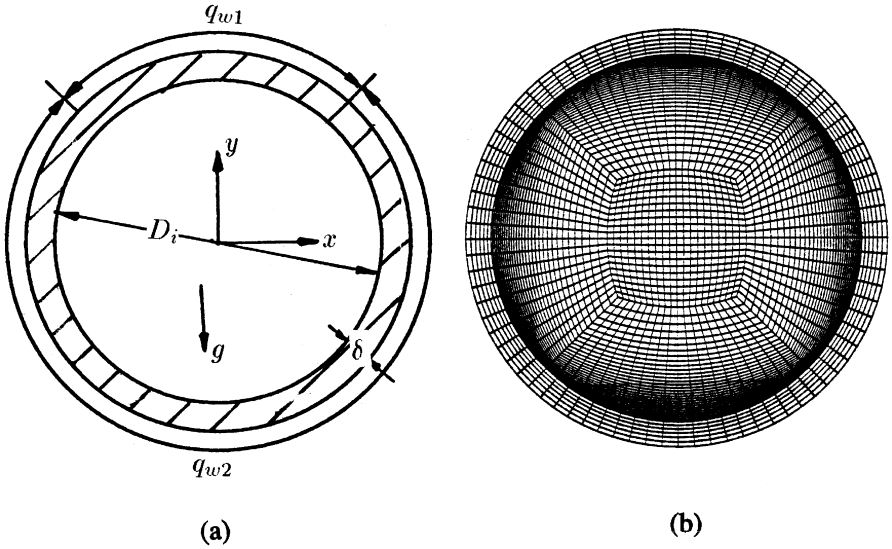

Fig. 1. Schematic of geometry and refined mesh.

$$\mu_t = C_\mu \rho \frac{k^2}{\varepsilon} \tag{5}$$

The two turbulent quantities k and ε satisfy the following transport relations at each point of the flow region:

$$\frac{\partial(\rho k)}{\partial t} + \frac{\partial(\rho u_j k)}{\partial x_j} = \frac{\partial}{\partial x_j}\left[\left(\mu + \frac{\mu_t}{\sigma_k}\right)\frac{\partial k}{\partial x_j}\right] + P + G - \rho\varepsilon \tag{6}$$

$$\frac{\partial(\rho \varepsilon)}{\partial t} + \frac{\partial(\rho u_j \varepsilon)}{\partial x_j} = \frac{\partial}{\partial x_j}\left[\left(\mu + \frac{\mu_t}{\sigma_\varepsilon}\right)\frac{\partial \varepsilon}{\partial x_j}\right] + C_1 \frac{\varepsilon}{k}(P + C_3 G) - C_2 \rho \frac{\varepsilon^2}{k} \tag{7}$$

where P is the shear production term defined by

$$P = (\mu + \mu_t)\frac{\partial u_i}{\partial x_j}\left(\frac{\partial u_i}{\partial x_j} + \frac{\partial u_j}{\partial x_i}\right) \tag{8}$$

and G accounts for the effect of the buoyancy force:

$$G = \frac{(\mu + \mu_t)}{\sigma_T}\beta g_j \frac{\partial T}{\partial x_j}. \tag{9}$$

For the container wall,

$$\frac{\partial T}{\partial t} = \alpha_w \frac{\partial^2 T}{\partial x_j^2}. \tag{10}$$

The values of the empirical constants in the model are [17, 18]

$C_\mu = 0.09 \quad C_1 = 1.44 \quad C_2 = 1.92 \quad C_3 = 1.0$

$\sigma_T = 1.0 \quad \sigma_k = 1.0 \quad \sigma_\varepsilon = 1.3.$

The CFX-F3D code [19], a general-purpose program for simulating laminar and turbulent flow and heat transfer, is utilized. The discretized equations are solved using the SIMPLEC [20] velocity-pressure coupling algorithm. The mesh, which is body-fitted to the geometry, is shown in Fig. 1(b). There are 94 non-uniformly-spaced meshes across the diameter, closely spaced near the wall, 80 uniformly-spaced meshes around the azimuth and there are 6 meshes in the container wall to capture the wall temperature profile. This mesh is found to be fine enough to produce mesh-independent solutions from trial calculations for several different mesh sizes. An adaptive, time-stepping option with automatic control of the time step is used, to optimize run-time efficiency.

3. Numerical results

In discussing results from the numerical simulation, emphasis is placed on the velocity and temperature fields in order to clarify the flow and heat transfer mechanisms. Figure 2 shows typical velocity vectors and (shaded) temperature contours at various times during the transient. At the initial stage of the heating, shown in Fig. 2(a), the temperature field in the fluid displays concentric circular profiles near the container wall, which shows that heat conduction dominates the heat transfer process. Note that there is heat conduction in the wall around the azimuth due to the different rates of heating on the outside, and non-uniformly-distributed wall temperature. The buoyancy force acting on the hot fluid boundary layer next to the wall drives the fluid inside the container upwards next to the curved wall and downwards through the core region, forming two counter-rotating symmetric vortices. Later, the core gradually becomes thermally-

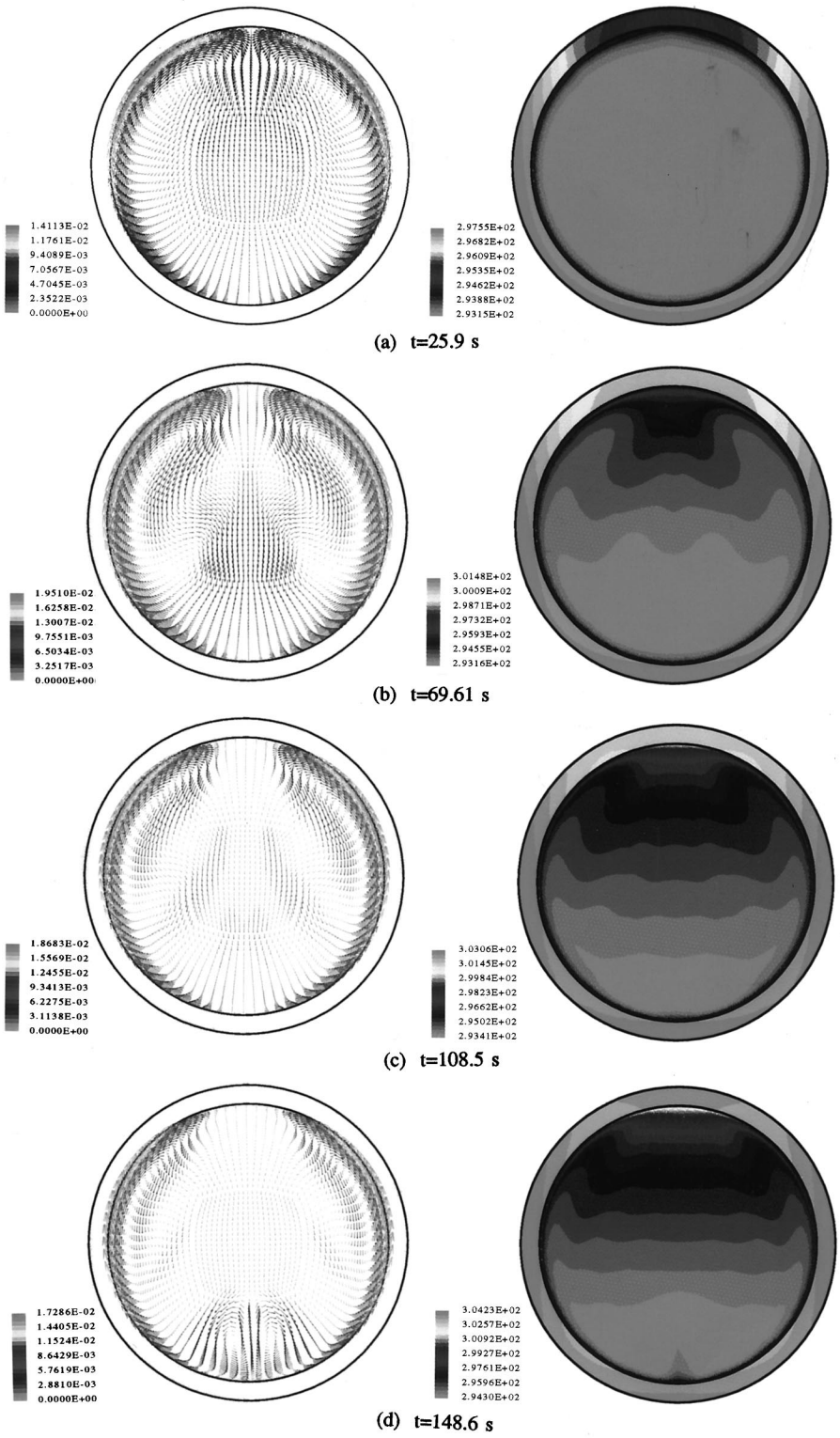

Fig. 2. Temporal evolution of velocity vectors (m s^{-1}) and shaded temperture contours (K). (a) $t = 25.9$ s, (b) $t = 69.61$ s, (c) $t = 108.5$ s, (d) $t = 148.6$ s, (e) $t = 173.3$ s, (f) $t = 400.1$ s, (g) $t = 1000.1$ s, (h) $t = 2200.1$ s.

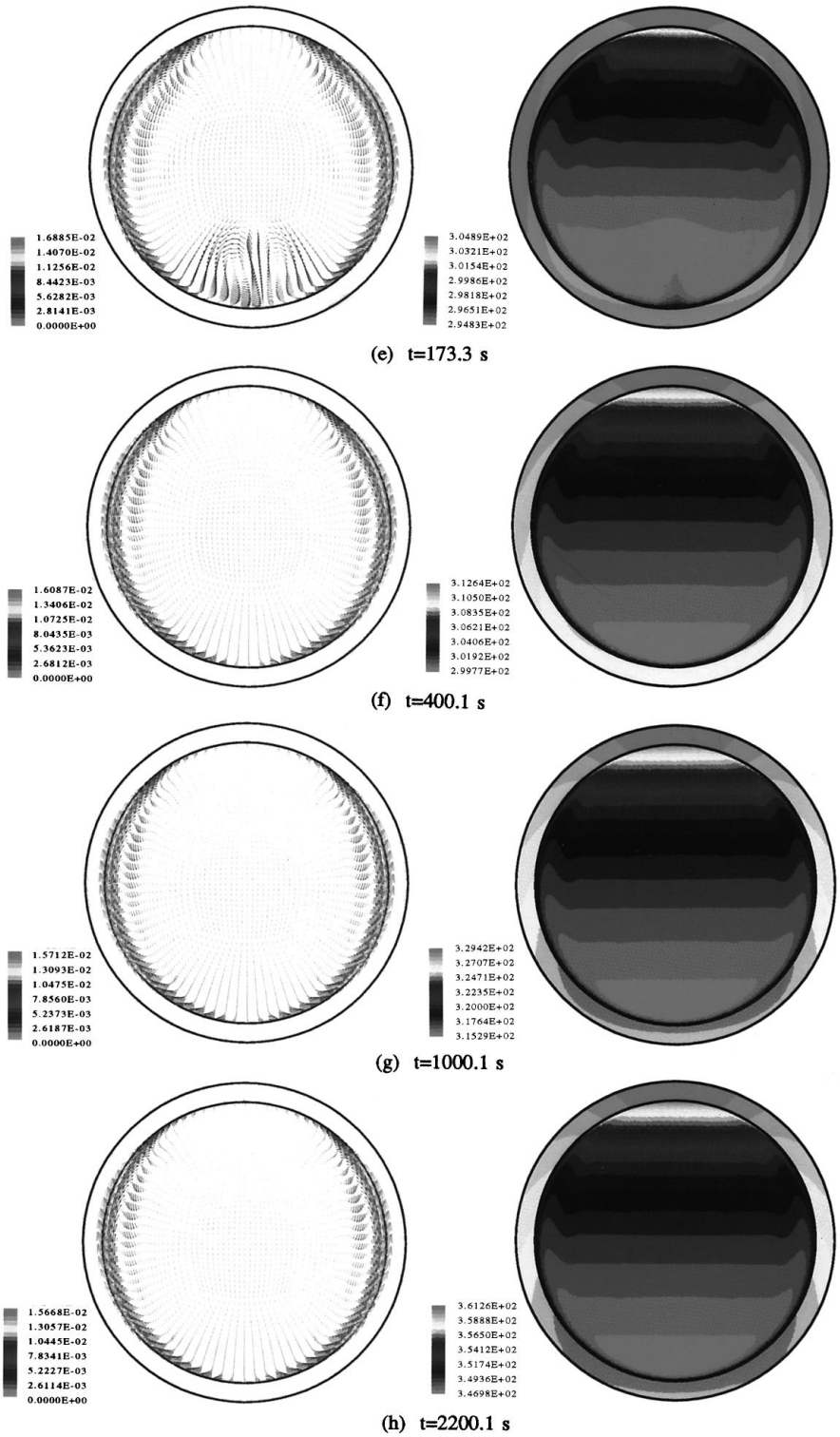

Fig. 2—*continued.*

stratified but relatively stagnant, with hot fluid near the wall continuously transported upwards, as shown in Figs 2(b) and (c). During this period, the highest wall temperature is still located at the bottom of the cylinder. The flow there then becomes rather complicated and a second pair of counter-rotating eddies is formed, which makes the flow and thermal fields slightly asymmetric near the bottom, but symmetric elsewhere in the flow domain. This four vortex flow pattern, shown in Figs 2(d) and (e), appears to be unstable and the two vortex pattern is soon reestablished with the thermal stratification in the core region strengthening during this developing period. The highest fluid temperature is located at the top of the vessel. At $t \approx 400.0$ s, the flow and heat transfer inside the container reach a quasi-steady state: the twin-vortex flow pattern prevails, the heat transfer coefficient remains nearly constant during the later phase of the transient, and well-developed thermal and velocity boundary layers are established. The fluid in the core region is relatively stagnant and strongly thermally stratified. The lowest fluid and wall temperatures occur near the bottom of the container and the highest wall temperature moves to the top.

The variation of the average temperatures of both the fluid and the wall with time is illustrated in Fig. 3. At the initial stage of the transient ($t < 100.0$ s), the average temperature of the container wall increases rapidly but the increase in the fluid temperature is more gradual. In other words, during this period, the imposed heat flux on the outside wall of the container mainly contributes to the increase of the internal energy of the wall. Once the motion of the fluid inside the container is established, the heat transferred from the wall to the fluid increases due to convection heat transfer and the rate of increase of wall temperature slows down. For $t > 100$ s or so, the change in average temperatures with time follows a linear law. When the flow and heat transfer inside the cylindrical container reaches quasi-steady state, the average temperatures of both the fluid and the wall increase at nearly the same rate and their difference approaches the constant value: $T_w - T_f \approx 8.0°C$. It should be mentioned that the linear increase of the wall temperature with time predicted by the present numerical simulation is consistent with the experimental results of Vatutin et al. [12] for air, and with our own for water, and with the lumped-parameter, analytical model of Xia, Smith and Yadigaroglu [16] for conjugate transient heat transfer in cylinders with volumetric heat sinks.

The parameter of practical interest in heat transfer simulations is the average Nusselt number Nu, which is defined in terms of the average temperature difference between the fluid and the wall:

$$Nu = \frac{D_i q}{\lambda(T_w - T_f)} \tag{11}$$

where q is the time-dependent, average wall heat flux into the fluid (which is not equal to the heat flux imposed on the outside wall of the container, as described later), T_w and T_f the average temperatures of both the wall and the fluid. The variation of the average Nusselt number with time is shown in Fig. 4. At early times there is a fluctuation but, for $t > 130$ s, Nu decreases monotonically until $T \approx 600$ s and thereafter asymptotes to the constant value of 262 (the corresponding average heat transfer coefficient is about 751 W m^{-2} K). It is found that the average heat flux from the inside wall surface to the fluid is about 6053 W/m^2 once the quasi-steady state is reached, while the average heat flux imposed around the outside surface of the wall is 6245 W m^{-2}. The difference between them accounts for the continuing increase of the internal

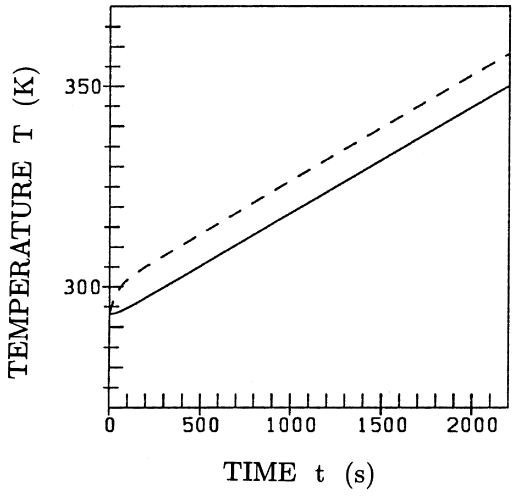

Fig. 3. Variation of average temperatures of both fluid and wall with time. --- T_w, — T_f.

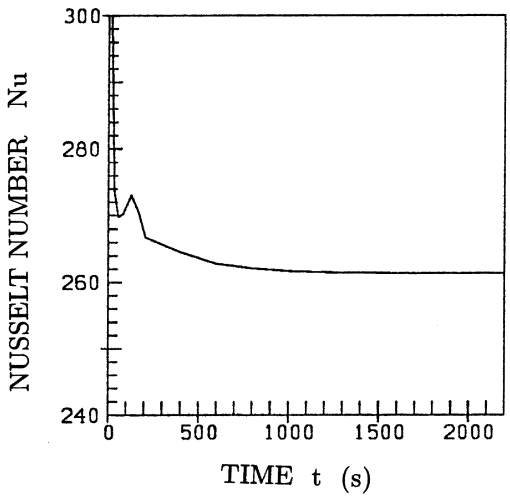

Fig. 4. History of the average Nusselt number.

energy of the container wall (Fig. 3). Thus, neglecting the influence of the wall (i.e., assuming zero-thickness wall) would overpredict the real heat transfer to the fluid by about 15% for the present physical model.

4. Description of experiment

The experimental setup, sketched in Fig. 5, consists of an aluminium cylinder with inner and outer diameters of $D_i = 220$ mm and $D_o = 250$ mm, respectively, and the length $L = 400$ mm. Two flanges fix round glass windows to the end openings of the tube. The cylinder is mounted horizontally on two thermally-insulating supports. On the top surface, three chimney-like ports containing channels of 110 mm in height, 140 mm in length and 10 mm in width, for probe access have been installed. Water can be transferred into the container, recirculated for cooling and drained again via several pipes during experiments. The ports also contain water. The container is heated from outside by mineral-insulated heating wires. On the lower three quarters of the cylinder surface, where the highest heat flux is applied, the wires are fixed in grooves parallel to the cylinder axis, whereas on the upper quarter and outside of the chimneys, they are held in place by bandages. Heating of the ports is necessary in order to establish a layer of hot water in the access slits to avoid natural convection heat transfer between cylinder and slits. The heating wires are connected to six separately-controlled power suppliers. Two of these feed the heaters on the top quarter of the cylinder and the ports. The container and the access ports are thermally insulated by a layer of thick mineral wool. Temperature is measured by calibrated thermocouples installed in the container wall with tips 1 mm off the inside surface and on movable probes inserted from above through the access slits, and recorded by means of a multichannel scanner. The experiments provide time-dependent temperature distributions in the water and the walls under condition of turbulent natural convection. A constant heat fluxes imposed on the outer surface of the container wall are those given in Fig. 1. The heating experiments were repeated several times at the same initial and boundary conditions with the movable thermocouples for scan-

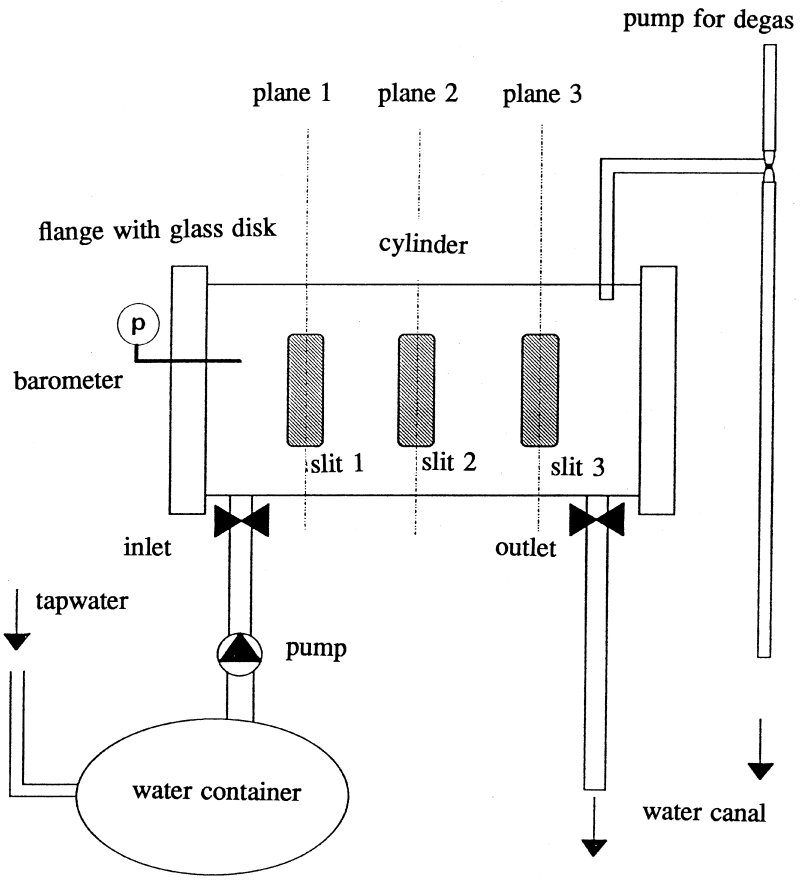

Fig. 5. Schematic of experimental setup.

ning the space-dependent temperature field in the fluid. In all the tests, the ports and the upper quarter of the container were first preheated for about 4 min. before switching on the power for the lower heating sections. This procedure was chosen to obtain stabilized stratification in the slits before onset of natural convection in the lower parts of the cylinder, as mentioned earlier.

The instrumentation used in the experiments was sufficient to detect possible 3-D effects in the fluid. With a ratio $L/D \approx 2$ being chosen, one may expect that two counter-rotating circulation rolls to develop, with horizontal axes normal to the container axis, and driven by the unstable stratification in the lower part of the container and by the heat losses to the end windows and flanges. The experiments, however, did not reveal any important effect of 3-D circulation effects, and only a slight variation of the temperature in the upper part of the container, along the axial direction, was detected. Evidently, natural convection inside the container is essentially two-dimensional, and boundary layer controlled. Heat balance calculation shows that there was about 25% heat loss during an experiment, the uncertainty in q_{w1} is estimated to be bout 20% and the uncertainty in thermocouple measurements was less than 0.1°C.

5. Experimental results

All temperature profiles quoted here are taken in the mid-plane normal to the container axis. In Fig. 6, the measured temperatures at various points are shown at three different times when the reference wall temperature reaches values of $T_{ref} = 50$, 60 and 70°C, referred to as states 1, 2 and 3, respectively; symbols like V27, V43 etc. denote the repeated tests at the same heating. The corresponding experimental times elapsed from the switching on of the main heaters are typically 900, 1400 and 1900 s (noting that the time taken to reach the first state at $T_{ref} = 50$°C differs up to 15% because the initial water temperature varies between 17–20°C). The three states lie well within the quasi-asymptotic domain of the numerical simulation. It is seen from Fig. 6 that the thermal field is well stratified.

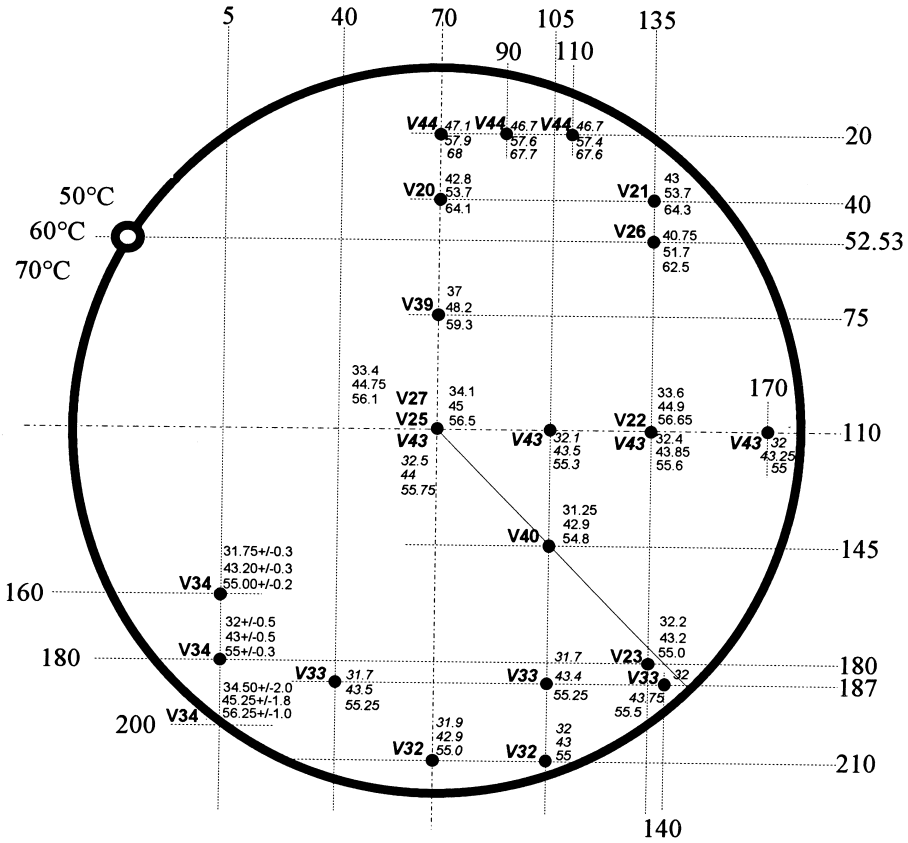

Fig. 6. Measured temperature profiles at mid-section.

6. Comparison of numerical and experimental data

Numerical results are compared against our experimental data in Figs 7(a), (b) and (c), which show local temperatures on two horizontal and three vertical planes at three times $t = 600$, 1000 and 1400 s, respectively. It is seen that agreement is satisfactory. The experimental data along the horizontal planes reveal that the core is strongly thermally-stratified, and the calculated temperatures reflect this behaviour. There exists some discrepancy in the top part of the container. This may be caused mainly by the three azimuthal slots in the upper surface of the container for inserting the thermocouple probes, resulting in a different heat flux from the numerically-given value in that region.

Furthermore, the average temperature difference between the wall and the fluid was 8.1°C obtained by averaging the measured temperatures at different

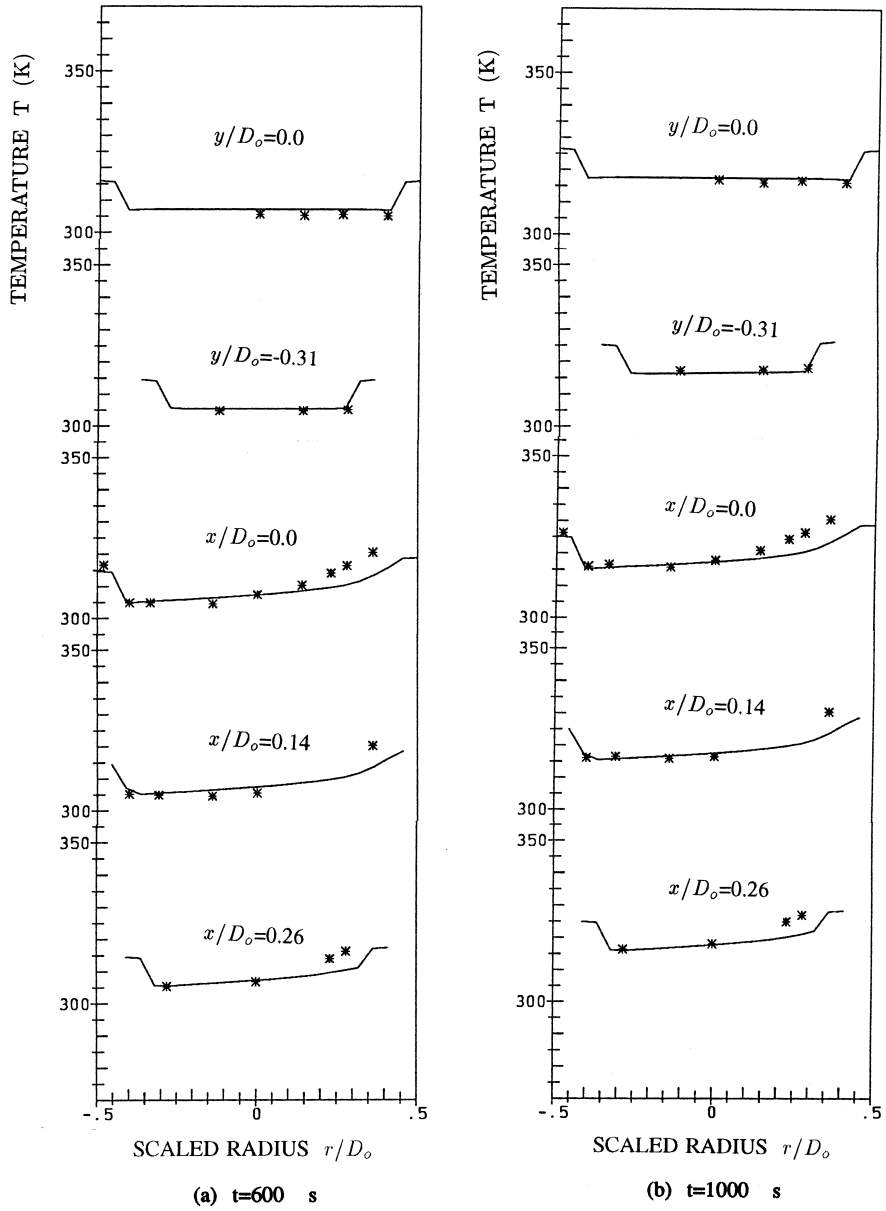

Fig. 7. Comparison of predicted local temperatures with experimental data at various times. — numerical, * experimental. (a) $t = 600$ s, (b) $t = 1000$ s, (c) $t = 1400$ s.

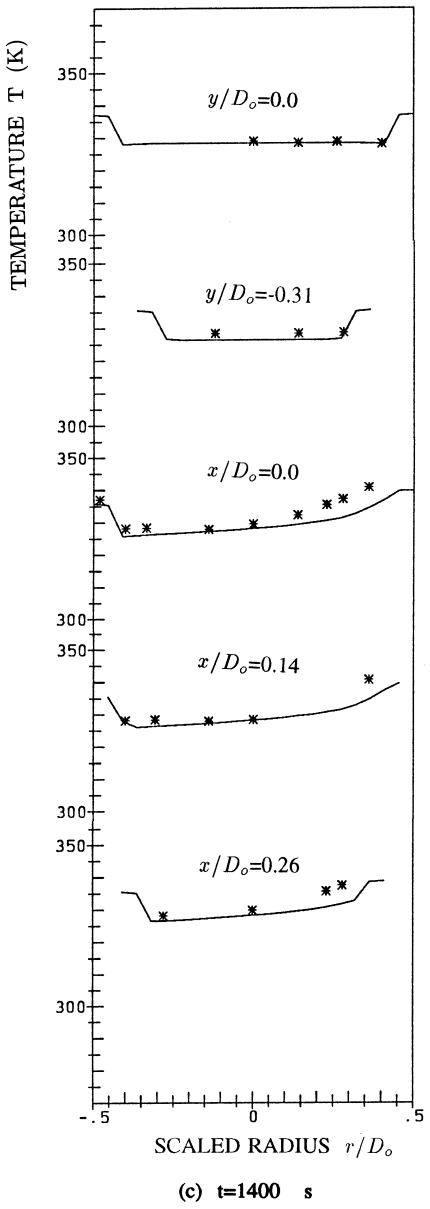

Fig. 7—*continued.*

locations while it is 8.0°C in quasi-steady state from the numerical prediction. Both are almost identical. It should be pointed out that the time interval from one state to next state is about 1.2 times in the experiments as large as that from the numerical predictions, which may be caused by the difference of boundary conditions and the influence of thermal properties.

It is also worth noting that, in quasi-steady state, the difference between the maximum and minimum wall temperature is about 4.3°C; the average temperature difference between the wall and the fluid is about 8.0°C; the difference between the maximum wall temperature and the minimum fluid temperature is about 19.0°C. Thus, the non-uniform profile of temperature around the container wall will have some influence on the heat transfer from the wall to the fluid. In other words, the assumption of a zero-thickness wall could lead to a misleading interpretation of the local heat flux along the wall. With the existence of the wall, the heat current is not radially directed due to the wall heat conduction and a part of heat imposed on the outer circumference of the container is needed for heating the wall.

7. Conclusions

A detailed numerical simulation of conjugate, transient, turbulent natural convection in a horizontal cylindrical container has been carried out. The main contributions of the present investigation are that (1) the study of transient natural convection in horizontal cylinders has been extended to the turbulent region, and (2) the influence of conduction in the container wall on the flow and heat transfer characteristics has been included. The numerical predictions show that the flow patterns during the transient evolve from a two-vortex to a four-vortex and back again to a two-vortex configuration. The four-vortex flow pattern appears to be unstable and is accompanied by asymmetric flow at the bottom of the container. Early in the transient, the temperature profile is concentric with the container wall, indicating a conduction-controlled heat transfer regime. Then convection, driven by buoyancy forces, prevails and the flow and temperature fields change with time. Later, a quasi-steady state is reached in which the wall-to-fluid heat transfer coefficient becomes nearly constant, the average temperatures of both the fluid and the wall increase linearly with time, their difference asymptoting to a constant,and the core is nearly-stagnant and strongly thermally-stratified.

The numerical predictions also reveal that the existence of the wall has some influence on natural flow and heat transfer. The heat transferred from the wall to the fluid is smaller than that nominally-imposed on the outside surface of the wall, and the assumption of a zero-thickness wall would then lead to overprediction of the heat transferred into the fluid. Furthermore, the internal wall surface temperature exhibits a strong non-uniformity because of heat conduction in the wall and the natural convection in the fluid; this in turn affects the profile of the local heat flux around the cylindrical surface.

Temperature measurements from a water experiment have been used to validate the numerical predictions. These confirm that the numerical model is accurately reproducing the principal flow and heat transfer mechanisms.

References

[1] Martini WR, Churchill SW. Natural convection inside a horizontal cylinder. AIChE J 1960;6:251.

[2] Sabzevari A, Ostrach S. Experimental studies of natural convection in a horizontal cylinder. Heat Transfer 1974;3:100.

[3] Brook IH, Ostrach S. An experimental investigation of natural convection in a horizontal cylinder. J Fluid Mech 1970;44:545.

[4] Deaver FK, Eckert ERC. An interferometric investigation of convective heat transfer in a horizonal fluid cylinder with wall temperature increasing at a uniform rate. Heat Transfer–1970, Paper NC 1.1. Elsevier Publishing, 1970;4.

[5] Weinbaum S. Natural convection in a horizontal cylinder. J Fluid Mech 1964;18:409.

[6] Ostrach S, Hantman, RG. Natural convection inside a horizontal cylinder. Chem Eng Comm 1981;9:213.

[7] Hellums JD, Churchill SW. Transient and steady state free and natural convection, numerical solutions, Part II—the region inside a horizontal cylinder. AIChE J 1962;8:692.

[8] Robillard L, Vasseur P, Nguyen HT. Thermal stratification induced by a periodic time-dependent temperature imposed on the boundary. J Heat Transfer 1987;109:525.

[9] Takeuchi M, Cheng K. Transient natural convection in horizontal cylinders with constant cooling rate. Waerme und Stoffuebertragung 1976;9:215.

[10] Leong SS, de Vahl Davis G. Natural convection in a horizontal cylinder. In Lewis RW, Morgan K, editors. Numerical Methods in Thermal Problems 1979;287.

[11] Xia, JL, Smith BL, Yadigaroglu G. Transient and steady buoyancy-driven flow in a horizontal cylinder. Applied Mathematical Modeling 1994;18(12):691.

[12] Vatutin IA et al. Vortical structure and temperature fields in unsteady-state natural convection with a horizontal tube. Experimental Heat Transfer 1993;6:69.

[13] Lee, JH, Park WH, Daguenet M. Theoretical study of the natural convection flows in a partially filled vertical cylinder subjected to a constant wall temperature. Proc 1987 ASME–JSME Thermal Eng Joint Conf 1987;4:1.

[14] Sun J, Oosthuizen PH. Transient natural convection in a vertical cylinder with a specified wall temperature. HTD 1988;96:107.

[15] Sun J, Oosthuizen PH. Transient natural convection in a vertical cylinder with a specified wall flux. HTD 1989;107:305.

[16] Xia, JL, Smith BL, Yadigaroglu G. Analysis of conjugate heat transfer in a cylinder with uniform heat sink. Heat Transfer 1994;2:473.

[17] Launder BE, Spalding DB. The numerical computation of turbulent flows. Comput Methods in Applied Mech Eng 1974;3:269.

[18] Rodi W. Turbulence models and their application in hydraulics, a state of the art review. Int Association for Hydraulics Research, Delft, 1980.

[19] CFX-F3D Release 4.1, User Guide, AEA Technology, Harwell, 1996.

[20] Van Doormal JP, Rathby GD. Enhancements of the SIMPLE for predicting incompressible fluid flows. Numer Heat Transfer 1984;7:147.